International Journal of Heat and Mass Transfer 71 (2014) 790–807

Contents lists available at ScienceDirect

International Journal of Heat and Mass Transfer

journal homepage: www.elsevier.com/locate/ijhmt

Determining the thermal conductivity of liquids using the transient hot disk method. Part II: Establishing an accurate and repeatable experimental methodology

Ronald J. Warzoha, Amy S. Fleischer *

Department of Mechanical Engineering, Villanova University, Villanova, PA 19085, United States

A R T I C L E   I N F O

Article history:
Available online 3 January 2014

Keywords:
Transient plane source
Thermal conductivity
Fluids
Nanofluids
Accuracy

A B S T R A C T

In this study, the accuracy of the conventional method that is employed to determine the thermal conductivity of fluids with the transient plane source (TPS) technique is evaluated experimentally using six different fluids. It was found that the accuracy of this method is insufficient for calculating the thermal conductivity of fluids due to: (1) the technique's inability to resolve the volumetric heat capacity in close proximity to the sensor, leading to highly erroneous calculations of thermal conductivity at early time scales, and (2) the lack of any means to predict whether the onset of natural convection will have an effect during testing. As a result, a new method is developed that utilizes the known volumetric heat capacity of a fluid and the equation used to predict the onset of natural convection that was developed in Part I of this study, which is published separately. Results suggest that this new method yields highly accurate calculations for the thermal conductivity of fluids (within 5.6% of values reported in the literature) over a wide range of Prandtl number ($Pr = 0.7–11,000$) and temperature.

1. Introduction

The transient plane source (TPS) thermal characterization technique is becoming an important tool for the determination of the thermal properties of a variety of materials [1–10] due to its robust design, rapid characterization time and for its ability to simultaneously measure the thermal conductivity and thermal diffusivity of complex materials, such as nanocomposites. However, when evaluating the thermal conductivity of liquids, the method's accuracy is found to be substantially lower than when used with solids due to buoyancy-related fluid movement over the sensor face [11,12]. The self-heating of the TPS sensor can create natural convective currents when long measurement times are used and thus measurement accuracy is strongly affected by the user-selected measurement period. To date, few studies have attempted to account for these effects [11–14], and most have overlooked them altogether [2,15,8,16]. It is therefore possible that existing nanofluid studies may report artificially high thermal conductivities when measured using the TPS instrument, confounding the fundamental understanding of the physical mechanisms that drive thermal transport at these length scales. Thus, it is the goal of this work to establish a simple, repeatable and accurate method for calculating the thermal conductivity of fluids when using the TPS instrument.

The TPS instrument uses a thin, electrically insulated resistive element (sensor) that serves as both a heat source and resistance temperature detector (RTD) [17]. When used to measure the thermal properties of solids, the sensor is sandwiched between two solid materials and a low current is applied across the resistive element in order to produce a constant heat flux at the sensor interface. The temperature increase of the sensor is recorded using a resistance measurement and is highly dependent on the surrounding material's thermophysical properties [17–20]. In principle, a large increase in the average temperature of the sensor with time indicates that the surrounding material is thermally insulating, while a small increase indicates that the surrounding material is thermally conductive.

In order to obtain accurate results using this method for solids, the sensor power and measurement period must be selected such that the thermal penetration depth into the sample must be less than the distance to the opposite edge of the surrounding material. Once the instrument is initialized, the temperature rise of the sensor as a function of time is recorded and is used to determine the thermal properties of the surrounding material by applying the fundamental transient heat conduction equation to the sensor geometry with a semi-infinite boundary condition (Eq. (1)).

$$k\nabla^2 T + \frac{Q}{\rho \cdot c_p} = \frac{\partial T}{\partial t} \tag{1}$$

---

* Corresponding author.
E-mail address: amy.fleischer@villanova.edu (A.S. Fleischer).

0017-9310/$ - see front matter © 2013 Elsevier Ltd. All rights reserved.
http://dx.doi.org/10.1016/j.ijheatmasstransfer.2013.10.062

In order to validate the semi-infinite boundary condition, the penetration depth (Δp) is computed (Eq. (2)) after each measurement.

$$\Delta p = 2\sqrt{\alpha \cdot t} \tag{2}$$

In Eq. (2), α represents the thermal diffusivity of the sample and t represents the measurement period as specified by the user. The measurement period is defined as the difference between the final time and the initial time of the measurement, which are selected by the user. This allows the user to selectively prevent the interfacial resistance between the sensor and the surrounding material from affecting the solution of the thermal conductivity according to Eq. (1). For fluid measurements, the interface resistance between the sensor and the fluid is generally negligible. As such, the initial time is generally considered to be the time at which power is applied to the sensor in this study. The final time is selected by the user in order to avoid reaching a thermal penetration depth that violates the semi-infinite condition.

The hot disk sensor itself is made of a double-spiral nickel foil wire and is coiled into a known number of "n" concentric rings with equal spacing. The double-spiral nickel foil wire is encapsulated in two 25 μm thick Kapton sheets for electrical insulation of the nickel foil wire. Using the geometry of the sensor, He [21] solved for the average transient temperature increase of the sensor using semi-infinite boundary conditions with conduction into the surrounding medium as the only heat transfer mode at the sensor-material interface. The solution to the average transient temperature increase of the sensor as a function of its geometry, the power loading level applied to the sensor and the surrounding material's thermal properties is given in Eq. (3). A full derivation of this equation and the methodology used to determine both k and α simultaneously can be found in [20].

$$\Delta T(\tau) = \frac{P_o}{\pi^{3/2} \cdot r \cdot \alpha} D(\tau) \tag{3}$$

where

$$D(\tau) = \frac{1}{n^2(n+1)^2} \int_0^{\tau} \frac{d\sigma}{\sigma^2} \sum_{k=1}^{n} k \sum_{l=1}^{n} l e^{-\left(\frac{k^2+l^2}{n^2}\right) / 4\sigma^2} \cdot I_0\left(\frac{kl}{2n^2\sigma^2}\right) \tag{4}$$

$$\tau = \frac{\sqrt{kt}}{r} \tag{5}$$

In Eq. (3), P_0 is the heating power applied to the sensor (W), r is the radius of the sensor (m) and α is the thermal diffusivity of the sample (m^2/s). $D(\tau)$ represents a dimensionless time function described by Eq. (4). In Eq. (4), n represents the number of concentric rings in the sensor element, τ is the dimensionless time constant (also known as characteristic time) described by Eq. (5), k is the thermal conductivity of the sample (W/m K), l is the length of the nickel foil wire (m) and σ is an integration variable, a description of which can be found in [21].

If the volumetric heat capacity of the surrounding material is known *a priori*, ΔT can be solved for as a function of $D(\tau)$, which produces a linear distribution when the constraints are properly met. The thermal conductivity can then be calculated using the slope of the line, which is equal to the coefficient $P_o/(\pi^{3/2} \cdot r \cdot k)$.

However, in many instances the volumetric heat capacity is unknown. When this is the case, multiple unknown variables remain in Eq. (3) (k and α), and it becomes necessary to use an iterative procedure to solve for each variable. ΔT and $D(\tau)$ are determined via experiment while α is varied over a wide range of values in order to establish linear correlation coefficients as a function of α. The thermal conductivity is then calculated according to the same procedure used to determine k when the volumetric heat capacity is known for each value of α. The reported value of thermal conductivity is the one that yields the highest correlation coefficient for a linear distribution as a function of α. This procedure highlights the complexity of the measurement and calculations of thermal conductivity when the volumetric heat capacity of a material is unknown and thus it is expected that there exists a strong correlation between measurement accuracy and heat capacity.

The use of the TPS method described here for the accurate measurement of thermal properties in solids has been discussed in detail [17–20,22]. For fluids, however, the application of this method may be insufficient to obtain accurate measurements of their thermal properties because the total measurement time must also be carefully chosen in order to avoid natural convection across the sensor face [23,13].

The conventional TPS measurement methodology that is currently used for calculating the thermal conductivity of nanofluids first requires that the user test the base liquid in order to determine a measurement time that yields a thermal conductivity to within 5% of reported values. This same measurement time is then used to test the thermal properties of derivatives of that fluid (i.e. when the fluid is saturated with nanoparticles, heated/cooled to different temperatures, etc.) [24–27]. For instance, Zhang et al. [24] studied the effect of carbon coated metal nanoparticles on the thermal conductivity of polyethylene glycol solutions. The authors determined that a measurement period of 10 s resulted in an accurate determination of the thermal conductivity of pure polyethylene glycol. As a result, a measurement period of 10 s was used to determine the thermal conductivity of the base fluid when saturated with nanoparticles.

However, as fluids are altered by nanoinclusions, so too are their thermophysical properties. Therefore, both the time to the onset of convection and the transient thermal gradient across the sensor will change with the addition of nanoparticles, and the accuracy of the measurement may be affected. Recent studies have highlighted the importance of avoiding buoyancy and natural convection during testing [11–14]; however, none of these studies have quantified the effect of buoyancy in such a way that the user can easily choose a TPS measurement time based on the fluid's thermophysical properties and the sensor power loading level. In fact, many studies do not report the measurement time used for the determination of the thermal conductivity of their fluids at all [2,15,8,16,26,28,29] and consequently, it is difficult to assess the accuracy of these results.

In order to develop an accurate and repeatable solution method for the determination of the thermal conductivity of fluids using the TPS method, experiments are conducted with the TPS 500 instrument (manufactured by Hot Disk AB). Tests are performed on a variety of fluids with well-defined thermophysical properties, including: deionized water, ethylene glycol, 50% deionized water/50% ethylene glycol, methanol, glycerin and acetone. In order to demonstrate the difficulty in achieving consistently accurate results for the thermal conductivity of fluids when utilizing the current TPS methodology, the thermal conductivity of each fluid is first experimentally determined assuming no advanced knowledge of the fluid's heat capacity. This data is analyzed in order to determine the effect of measurement time on accuracy using the current solution procedure.

These experiments are then repeated using each fluid's known heat capacity in order to calculate thermal conductivities according to Eq. (3)without the need for iteration. The results from the two methods are compared to determine if the iterative procedure commonly used when heat capacity data is unavailable (as for new liquids) is able to provide an accurate thermal conductivity measurement.

The second part of this study investigates the role of natural convection on the accuracy of the solution across a wide range of measurement times and the third part of this study examines the effect of sensor power and sensor temperature rise on the accuracy of the thermal conductivity measurements.

Finally, these results are used to develop two new TPS measurement methodologies for determining the thermal conductivity of complex fluids with acceptable accuracy. The first solution procedure is applicable to fluids of known heat capacity and produces values of thermal conductivity that are within 5.6% of those reported in the literature. The second solution procedure is applicable to fluids of unknown heat capacity and produces values of thermal conductivity to within 14.9% of those reported in the literature. These methodologies will be shown to greatly improve the measurement accuracy over existing procedures and thus will allow for the expansion and further application of the TPS technique to complex, Newtonian fluids with confidence.

2. Experimental methods

In this study, a transient plane source Thermal Constants Analyzer (model TPS 500) is used to test the validity of the current solution procedure for determining the thermal conductivity of fluids with the TPS instrument and is then used to establish a more accurate procedure based on these results. Upon initialization, power is applied to the sensor element (i.e. across the concentric rings) when it is sandwiched between two semi-infinite materials and the resistance across the sensor is measured as a function of time. The resistivity of nickel is used to convert the resistance into a temperature and a temperature–time variation is subsequently used to solve for the thermal conductivity and volumetric heat capacity according to Eq. (3).

The sensor is suspended vertically within a liquid sample that is contained within a cylindrical vessel made of oxygen-free high conductivity (OFHC) copper, as shown in Fig. 1. Vertical orientation of the sensor was chosen for several specific reasons. Many of the accessories available for the sensor necessitate a vertical orientation [30], and as such many users are likely to implement the sensor in this way. Although the argument may be made that natural convection is easier to avoid if the sensor is in the horizontal orientation, natural convection currents will still occur across the sensor face in most horizontal cases. As natural convection is easier to quantify and control in the vertical orientation, this sensor position is preferred for greater accuracy. Finally, it is paramount that the sample not be contaminated when immersed in a bath. Thus, it is easier for most researchers to insert the sensor vertically into a sample than to design a leak-proof container that allows horizontal immersion into a liquid sample, as a vertical orientation does not require full submersion of the sample into a thermal bath.

Oxygen-free high conductivity copper ($k_{OFHC} = 390$ W/m K) is used to spread heat evenly throughout the container and create an isothermal condition in the sample. The copper vessel is partially immersed in a constant temperature thermal bath, which allows the user to precisely control the sample temperature. The sensor used in this study is the smallest sensor available for the TPS 500 instrument and has a radius of 3.189 mm. The smallest sensor is commonly used because it requires a smaller sample size for testing, which can substantially lower expenses when measuring the thermal conductivity complex fluids (such as nanofluids).

Upon test initiation, the sensor produces a constant heat flux and the temperatures of both the sensor and the surrounding fluid begin to increase. The surrounding fluid must behave as a semi-infinite solid and must not begin to convect during the measurement period. The container is therefore sized to allow heat to diffuse 5.1 mm in the radial direction and 9.4 mm in the axial direction without reaching another material or system boundary. Eq. (2)can be used to determine the total thermal penetration depth into the sample after the thermal conductivity is calculated and is used to ensure that the semi-infinite condition is met. The sensor and vessel geometries are listed in Table 1.

In order to avoid natural convection over the sensor face during testing, a measurement period must be chosen such that it is less than the time to the initiation of significant natural convection currents. This time can be calculated using the method established in the first part of this study [31] and is given by Eq. (6).

$$t_{onsetCV} = (9.525e^{-6} \cdot s \cdot W^{0.791} \cdot K^{-0.830}) \cdot \left(\frac{\mathrm{Pr}^{0.456} \cdot \mathrm{Ra}^{0.285}}{Q^{0.791} \cdot \beta^{0.830}} \right) \tag{6}$$

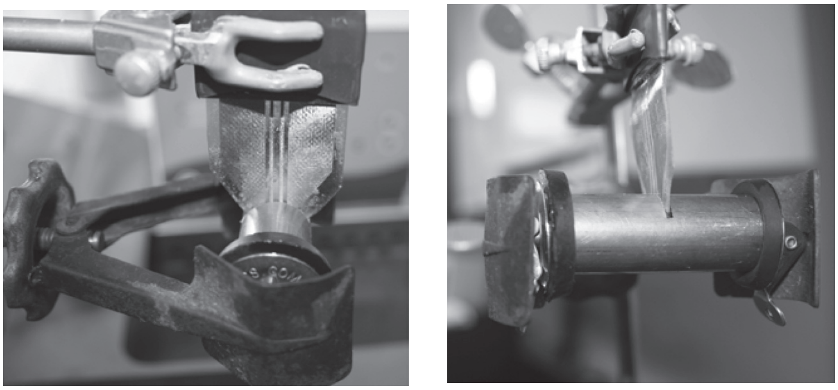

(a) Front view of sensor

(b) Side view of copper vessel

Fig. 1. TPS sensor immersed vertically in oxygen-free high conductivity copper vessel and constant temperature thermal bath.

Table 1
TPS 500 sensor and vessel geometry.

Vessel material	Vessel thermal conductivity (W/m K)	Inner diameter (mm)	Inner length (mm)	Maximum allowable radial thermal penetration depth (mm)	Maximum allowable axial thermal penetration depth (mm)
OFHC	390.0	16.57	18.9	5.1	9.4

Table 2
Thermophysical properties of fluids used in this study at 295 K.

Fluid type	k (W/m K)	ρ (kg/m^3)	c_p (J/kg K)	ν (m^2/s)	β (1/K)	Prandtl number
Deionized water (DI) [32]	0.606	997.3	4181	9.33×10^{-7}	2.27×10^{-4}	6.62
Ethylene Glycol (EG) [32]	0.251	1117	2391	5.76×10^{-5}	6.50×10^{-4}	2.28×10^{2}
50% DI/50% EG [32]	0.410	1046	3292	1.15×10^{-5}	4.38×10^{-4}	0.96×10^{2}
Acetone [32]	0.160	785	2180	4.10×10^{-7}	1.43×10^{-3}	4.32
Methanol [32]	0.2035	792	2545	7.45×10^{-7}	1.18×10^{-3}	7.38
Glycerin [32]	0.286	1263	2397	1.05×10^{-3}	4.70×10^{-3}	1.11×10^{4}

Should the test include time periods over which natural convection exists, the resultant solution for the thermal conductivity of the surrounding liquid will be artificially high. Thus, Eq. (6)was developed in order to ensure that the period over which the measurement is taken does not include the effects of natural convection.

The TPS 500 system allows the user to set the measurement time and has 11 time periods available for selection, each twice as long as the previous time period (2.5, 5, 10, 20, 40, 80, 160, 320, 640, 1280 and 2560 s). It is expected that greatest accuracy will occur by maximizing the measurement time (and thus the number of data points collected) without creating a situation where significant convection occurs. This study will test and quantify the effect of measurement time on the accuracy of the results.

The fluids used in this study and their corresponding thermophysical properties at room temperature (295 K) are listed in Table 2. These fluids are used to represent a wide range of Prandtl numbers such that the time to the onset of natural convection varies widely as a function of the fluid's viscosity and thermal properties.

In order to develop an accurate and repeatable solution method for the calculation of the thermal conductivity of fluids using the TPS method, a series of experiments are conducted on the fluids listed in Table 2.

2.1. Evaluation of the conventional TPS methodology used to calculate thermal conductivity

In order to determine the accuracy of the current solution methodology, a series of experiments are conducted. In the first experiment, the temperature of deionized water is increased from 290 to 320 K in increments of 10 K using a constant temperature thermal bath in order to alter its thermophysical properties. The effect of the variations in the fluid's thermophysical properties on the measurement accuracy is then quantified. The variability in fluid properties as a function of temperature is similar to the variation that occurs when mixing fluids or otherwise changing the fluid such as with nanoparticle suspensions. In order to further quantify the accuracy of the current solution methodology, the fluids listed in Table 2 are also tested at room temperature.

2.2. Effect of known volumetric heat capacity and the onset of natural convection on conventional methodology accuracy

The effect of knowing the volumetric heat capacity of a fluid *apriori* is analyzed in order to understand its influence on the conventional methodology's accuracy. Despite its important role in the determination of liquid phase thermal conductivity using the TPS technique, as highlighted in Eqs. (3) and (4), the volumetric heat capacity of fluid mixtures or of fluids with particulate suspensions often goes unreported in work that uses the TPS instrument [2,7,14,16,24–26,28]. Given that common equipment and procedures can be used to determine the volumetric heat capacity of fluids in advance of the TPS measurement, it is important to understand whether knowledge of the fluid's volumetric heat capacity *apriori* can enhance the TPS accuracy.

2.3. Effect of sensor power and sensor temperature rise on measurement accuracy

The selection of the sensor power by the user is directly related to the sensor temperature rise (i.e. higher powers can create localized temperature gradients in the surrounding liquid) and can directly affect solution accuracy. In fact, if the temperature rise of the sensor is sufficiently large and the liquid has thermophysical properties that are strongly affected by temperature, then the thermal conductivity measurement of the liquid as calculated by Eqs. (3) and (4) is more closely correlated to the sensor temperature than the bulk fluid temperature. In this study, several of the fluids listed in Table 2 are tested as a function of both temperature and sensor power in order to quantify the effect of sensor temperature rise on the solution of the thermal conductivity. Using these results, guidelines for the selection of sensor power are established.

2.4. Establishment of an accurate and repeatable solution method to determine the thermal conductivity of fluids using the TPS thermal characterization technique

In this work, an accurate and repeatable solution method is constructed for fluids with both known and unknown volumetric heat capacity. The new solution methods are designed to avoid both natural convection during testing and a sensor temperature rise that is too large for the accurate calculation of the thermal conductivity of fluids. These methods are based on an iterative scheme that uses known values of the fluid's thermal expansion coefficient and viscosity, both of which can be obtained by simple experimentation. The new methods are validated for all of the fluids listed in Table 2 at room temperature (295 K).

3. Results and discussion

3.1. Evaluation of the accuracy of the conventional TPS methodology when applied to determination of the thermal conductivity of liquids

In the first part of this study, the accuracy of the current methodology used to determine liquid phase thermal conductivity using the TPS thermal characterization technique is analyzed. As mentioned previously, the conventional TPS method first determines a measurement time that yields an accurate calculation for a fluid with known thermal conductivity. This same measurement time is subsequently used to test a derivative of the base fluid (such as a nanofluid). However, the base fluid properties are altered by the presence of nanoinclusions and thus the time to the onset of convection and the transient thermal gradient across the sensor will change, affecting the accuracy of the measurement. As the nanofluid properties are unknown, this introduced inaccuracy is also unknown and often unapparent to the user.

The TPS software allows the user to set the measurement time period to between 2.5 and 2560 s, as noted in the Experimental Methods section. For each fluid in Tables 3 and 4, a series of measurements of thermal conductivity were made using the TPS 500 at each available measurement period less than $t_{onsetCV}$. During each

Table 3
Thermophysical properties of DI water as a function of temperature [32].

DI water temperature (K)	k (W/m K)	ρ (kg/m^3)	c_p (J/kg K)	ν (m^2/s)	β (1/K)	Prandtl number
290	0.598	997.8	4184	9.79×10^{-7}	1.74×10^{-4}	7.56
300	0.613	995.1	4179	7.81×10^{-7}	2.76×10^{-4}	5.83
310	0.628	991.8	4178	6.40×10^{-7}	3.61×10^{-4}	4.62
320	0.640	987.6	4180	5.38×10^{-7}	4.36×10^{-3}	3.77

Table 4
Time to the onset of convection for each test fluid calculated per Eq. (6).

Fluid type	Fluid temperature (K)	P_0 (W)	$t_{onsetCV}$ (s)
Deionized water	290	0.1	4.71
Deionized water	300	0.1	3.42
Deionized water	310	0.1	2.77
Deionized water	320	0.1	2.37
Ethylene Glycol (EG)	295	0.1	6.69
50% DI/50% EG	295	0.15	4.50
Acetone	295	0.25	1.59
Methanol	295	0.15	2.26
Glycerin	295	0.05	21.5

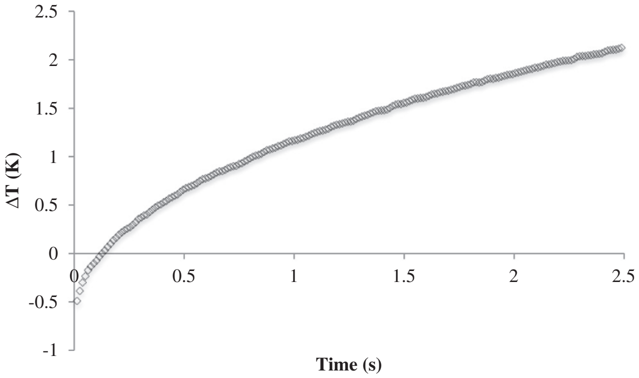

(a) 2.5 s measurement period

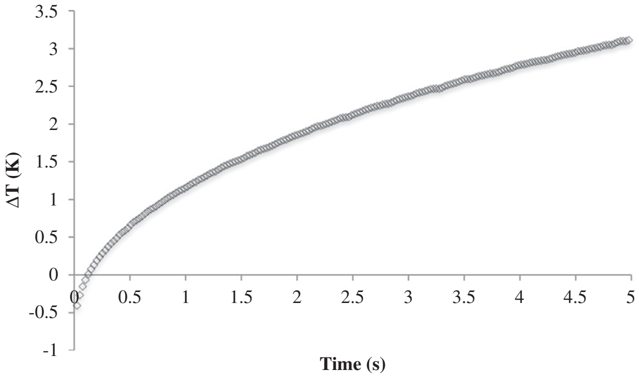

(b) 5 s measurement period

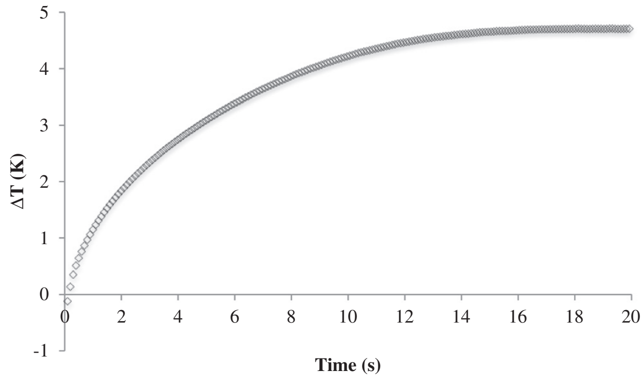

(c) 20 s measurement period

Fig. 2. Temperature vs. time for TPS sensor ($r = 3.189$ mm) immersed in Ethylene Glycol at $P_0 = 0.1$ W and $T = 300$ K.

measurement period, 200 temperature data points were recorded at uniform time intervals as illustrated in Fig. 2(a)–(c) for Ethylene Glycol at measurement periods of 2.5, 5 and 20 s. It should be noted that "measurement period" is defined as the total length of time that a test is conducted, while a "measurement time" is defined as any one of the 200 data points that are collected during testing.

In Fig. 2, ΔT represents the average temperature difference between the sensor and the surrounding bulk fluid, which is used to calculate its thermal conductivity and thermal diffusivity according to Eqs. (3) and (4). Fig. 2(c) shows that a 20 s measurement period experiences steady-state natural convection ($d\Delta T/dt = 0$) across the sensor as t approaches 20 s while the shorter measurement time intervals do not exhibit natural convection, making them a better choice for implementation. This illustrates the importance of properly choosing the measurement period.

The thermal conductivity of DI water is next measured as a function of temperature in order to determine whether the measurement time used to calculate the base fluid's thermal conductivity at room temperature ($T = 290$ K) can also be used to calculate its thermal conductivity when its thermophysical properties are changed. As defined earlier, the measurement period is the difference between the final time and the initial time of measurement, which are selected by the user. The initial measurement time is not necessarily the time at which the sensor is powered, but may be at some point after the power is applied, which allows the user to selectively prevent the interfacial resistance between the sensor and the surrounding material from affecting the solution. For fluid measurements, the interface resistance between the sensor and the fluid is generally negligible. Thus, for each case presented here the initial measurement time is $t = 0$ s. The final measurement time (herein referred to simply as 'measurement time') is the point that is altered to obtain thermal conductivity as a function of time during each measurement period (as shown in Figs. 3–14). The thermal conductivity of DI water is calculated as a function of measurement time for four different temperatures (290, 300, 310 and 320 K) in Fig. 3.

The distributions in Fig. 3(a)–(d) exhibit substantial variability in the calculated value of thermal conductivity as a function of both bulk fluid temperature and measurement time for DI water. Very few of the measurements are an accurate determination of the thermal conductivity (within ±5% of the reported values in the literature). For example, as seen in Fig. 3(a) an accurate determination of the thermal conductivity of DI water at 290 K depends both on the measurement time selected and on the total measurement period used. It can be seen in Fig. 3(a)–(d) that the periods over which the results are accurate are very small in comparison to the total measurement periods used (2.5, 5 and 10 s). Outside of these small measurement intervals during which the solution can be considered accurate, it is clear that the measured

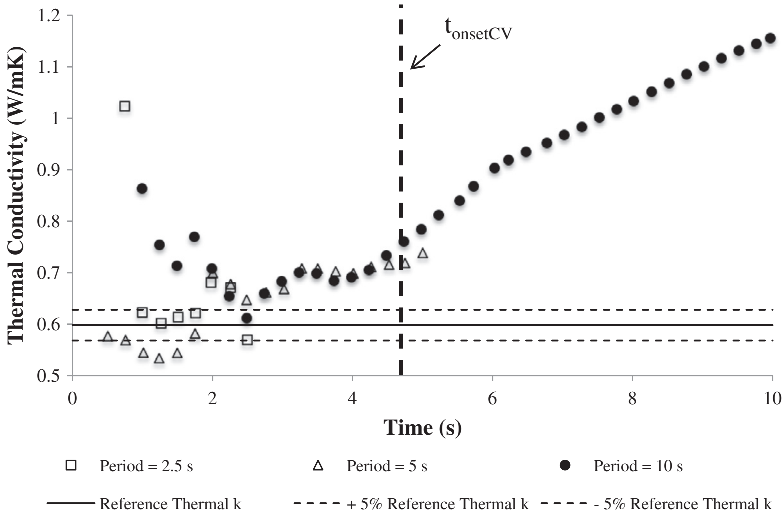

(a) DI Water at 290 K

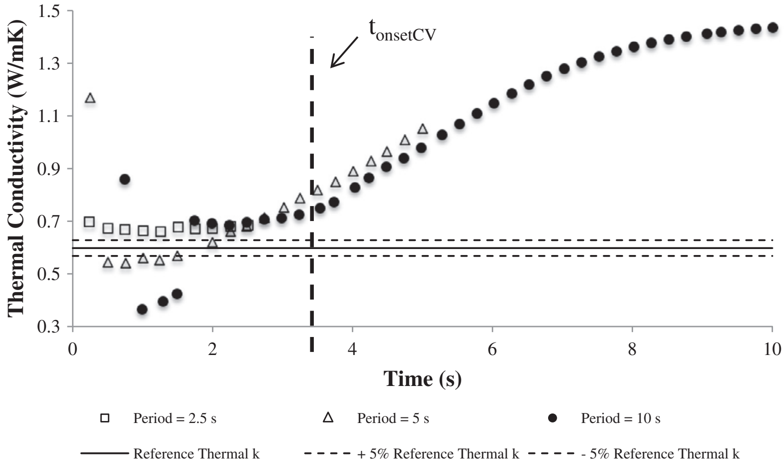

(b) DI Water at 300 K

Fig. 3. Thermal conductivity of DI water as a function of measurement time and temperature using the current methodology at $P_0 = 0.1$ W.

thermal conductivity values are highly erroneous with respect to measurement time due to the difficulty in resolving the volumetric heat capacity of the fluid, which results in a non-linear correlation for ΔT as a function of $D(\tau)$ when evaluated using Eqs. (3) and (4).

Additionally, it is clear from Fig. 3(a)–(d) that the measurement time at which the calculated thermal conductivity falls within an acceptable range of accuracy (±5% in reference to literature values) is different when the temperature is changed. This indicates that the conventional methodology is not sufficiently accurate for determining the thermal conductivity of fluids which have been altered from their base state (such as nanofluids). For instance, one might choose 1.5 s as the measurement time for a DI nanofluid based on the accurate determination of DI thermal conductivity in Fig. 3(a). If this measurement time were then used for the cases in Fig. 3(b)–(d), the reported thermal conductivities of the other fluids (DI water at 300, 310 and 320 K) would be artificially high (by as much as 150% above their true values according to these results). This indicates that studies which have used this methodology in the past [24–27] in order to determine the thermal conductivity of nanofluids may report values which are artificially high or low, depending on the measurement time chosen by the user.

In order to verify that the variability in the calculated thermal conductivity is not limited to one particular fluid, the remaining fluids in Table 2 are tested at room temperature ($T = 295$ K) using different measurement times. The results for each fluid are shown in Figs. 4–8. In each figure, the data remain highly variable across all data sets, regardless of the fluid type. It has previously been suggested that so long as measurement times are small, the current methodology can avoid the effects of natural convection [16–20,24–27] and thus obtain an accurate solution. While it is true that the onset of natural convection can be avoided so long as Eq. (6)is used for confirmation, it is clear that there is still great variability in the results across early time scales and that few readings fall in the acceptable accuracy range (±5% when compared to values presented in the literature). This remains true even for viscous fluids with high Prandtl number, such as Glycerin (Fig. 8). Interestingly, the solution for the thermal conductivity of glycerin converges after an initially scattered set of results. This isolated phenomenon is explained in a subsequent section. These results make abundantly clear that: (a) the current solution methodology is likely to produce inaccurate results for base fluid derivatives and (b) there is great difficulty in resolving the volumetric heat capacity of the fluid in close proximity to the heat source when using the current solution methodology.

Figs. 4–8 also reveal the importance of buoyancy-related effects on the solution of Eq. (3)for fluids. In Figs. 3–7, it can be seen that

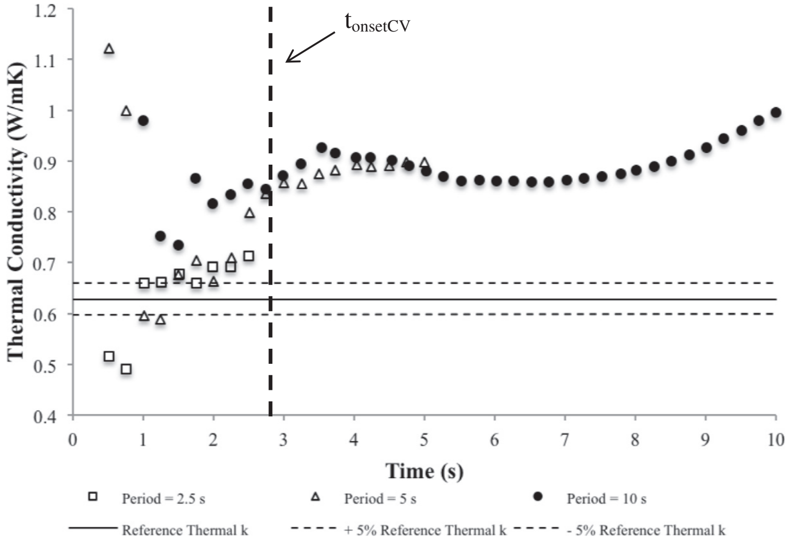

(c) DI Water at 310 K

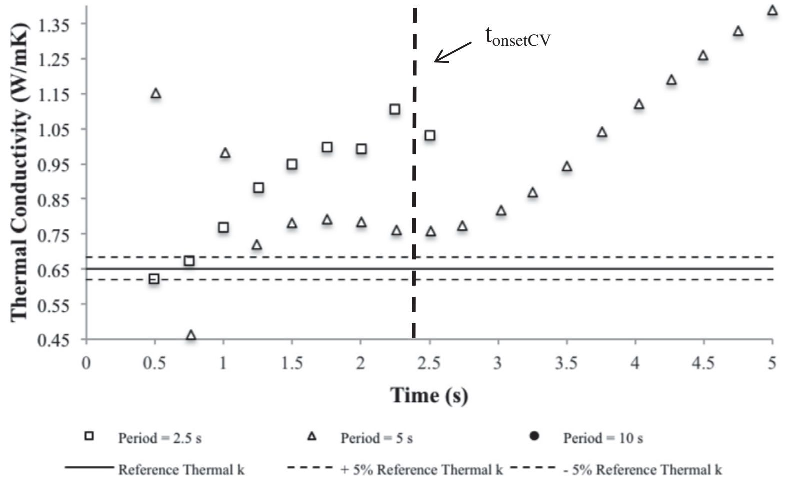

(d) DI Water at 320 K

Fig. 3 (*continued*)

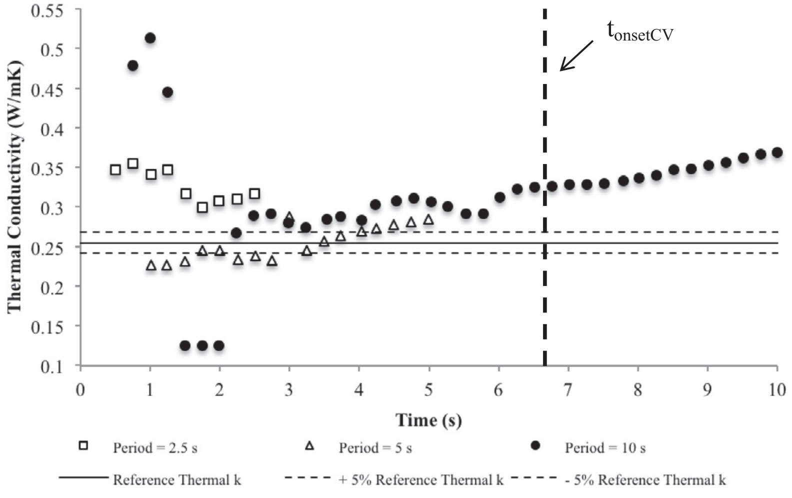

Fig. 4. Thermal conductivity of Ethylene Glycol at 295 K and $P_0 = 0.15$ W.

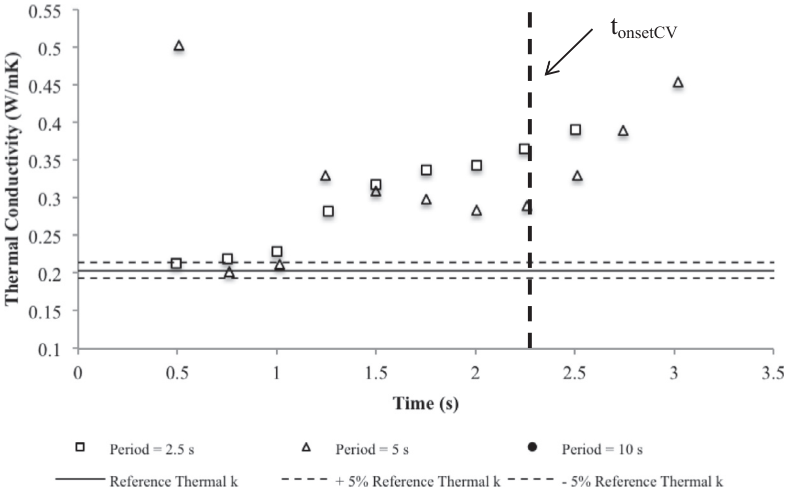

Fig. 5. Thermal conductivity of Methanol at 295 K and $P_0 = 0.15$ W.

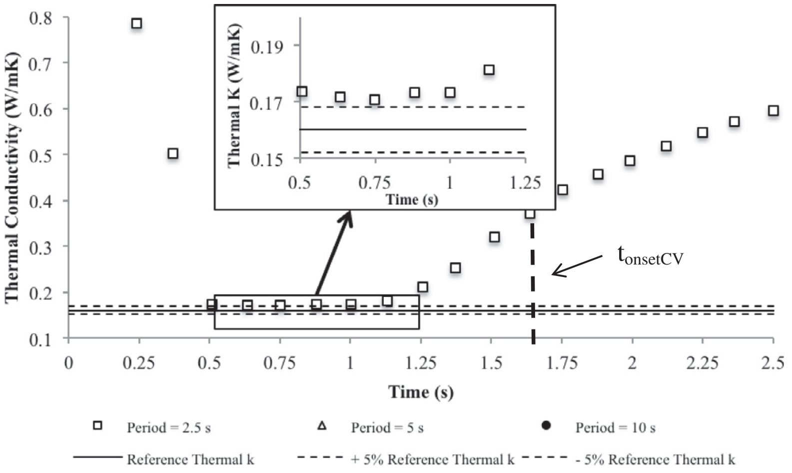

Fig. 6. Thermal conductivity of Acetone at 295 K and $P_0 = 0.25$ W.

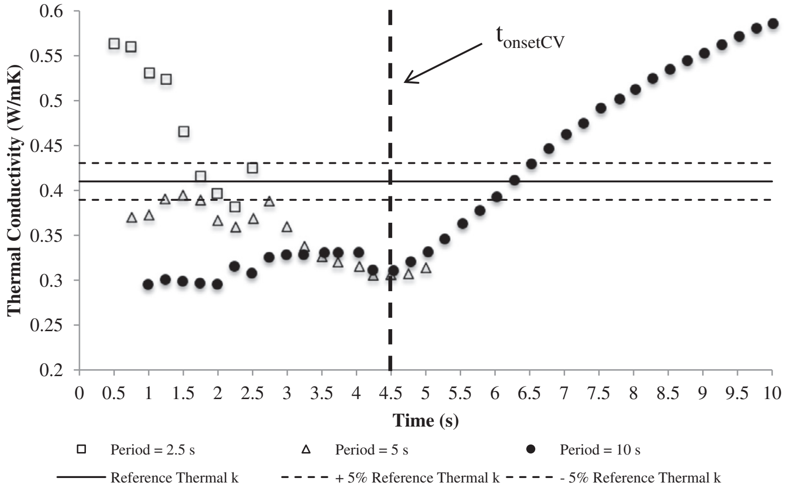

Fig. 7. Thermal conductivity of 50/50 DI water/Ethylene Glycol at 295 K and $P_0 = 0.15$ W.

for the long measurement times, there is a point at which the reported thermal conductivity begins to significantly rise. Not coincidentally, this point is found to be close to the time to the onset of natural convection for each of the fluids listed in Table 4. Thus, the combination of buoyancy effects and the difficulty in obtaining the volumetric heat capacity in close proximity to the sensor face(s)

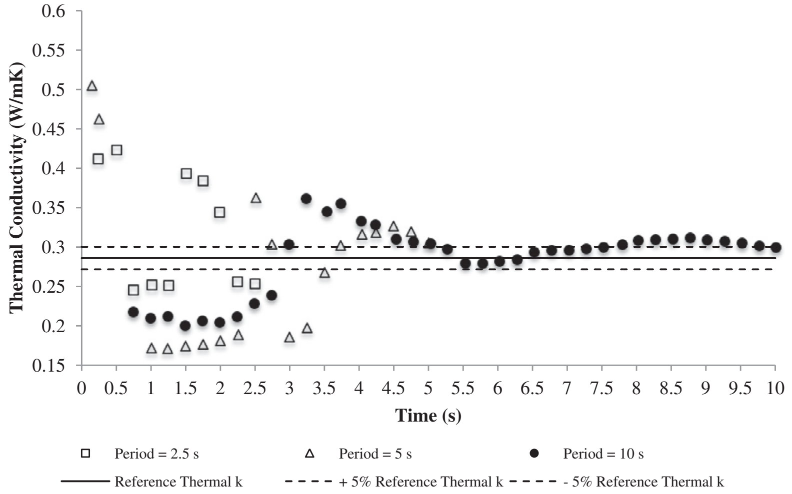

Fig. 8. Thermal conductivity of Glycerin at 295 K at $P_0 = 0.05$ W.

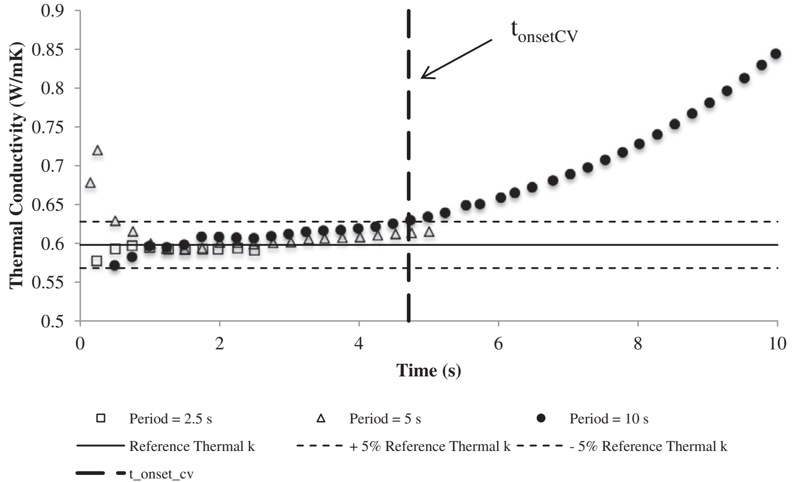

(a) DI Water at 290 K

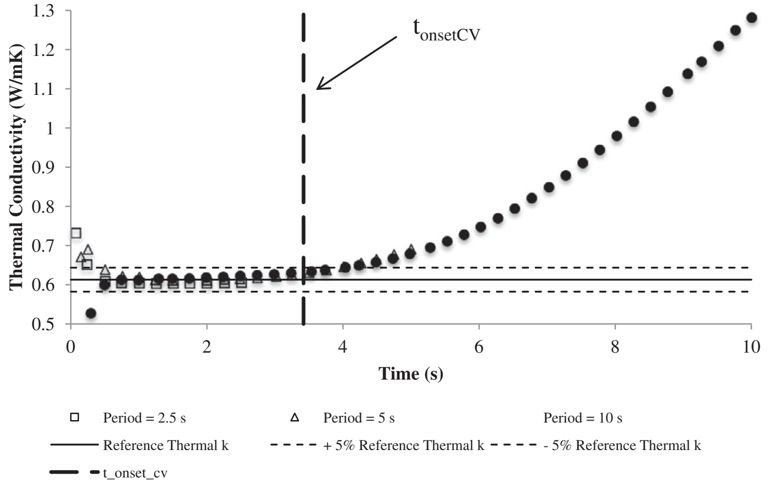

(b) DI Water at 300 K

Fig. 9. Thermal conductivity of DI water as a function of measurement time and temperature using the current methodology with known volumetric heat capacity at $P_0 = 0.1$ W.

result in a very short duration of time over which the reported thermal conductivity values are accurate for fluids with low Prandtl numbers. In Fig. 8, it is clear that at high Prandtl numbers (greater than the maximum used to generate Eq. (6)), there exists an extended period of time prior to natural convection and after some initial time interval over which the volumetric heat capacity

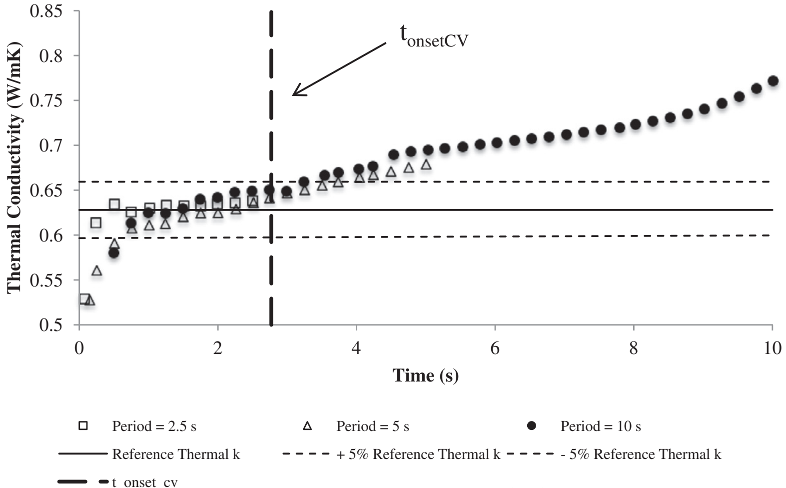

(c) DI Water at 310 K

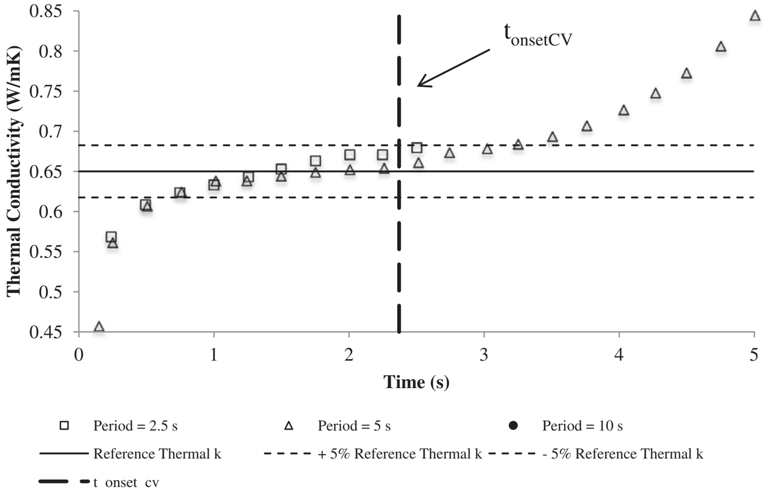

(d) DI Water at 320 K

Fig. 9 (*continued*)

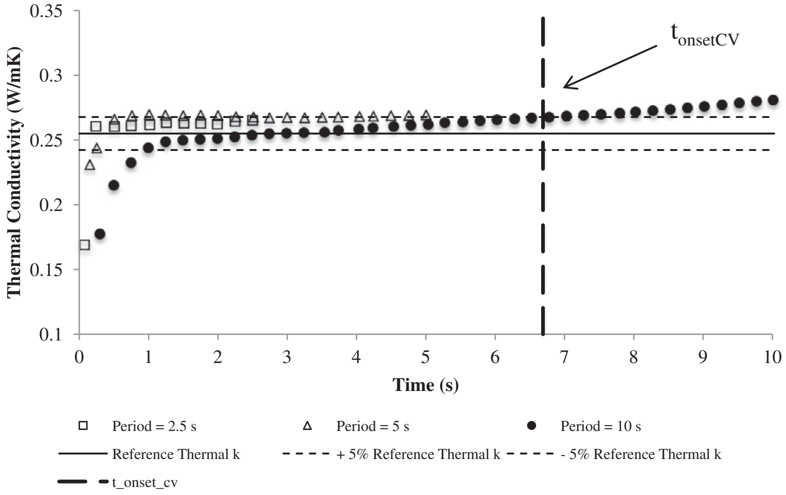

Fig. 10. Thermal conductivity of Ethylene Glycol at 295 K and $P_0 = 0.1$ W.

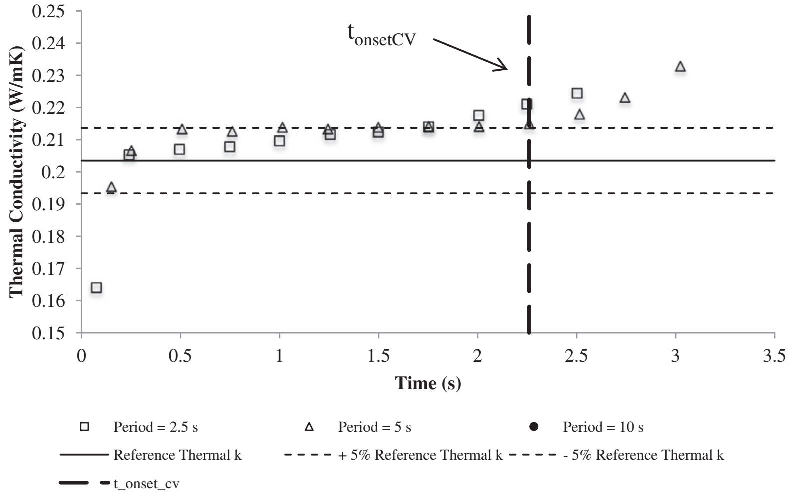

Fig. 11. Thermal conductivity of Methanol at 295 K and $P_0 = 0.15$ W.

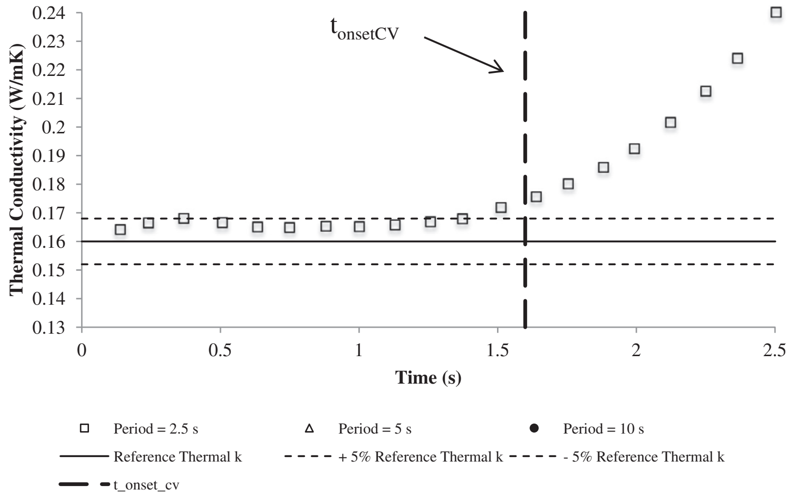

Fig. 12. Thermal conductivity of Acetone at 295 K and $P_0 = 0.25$ W.

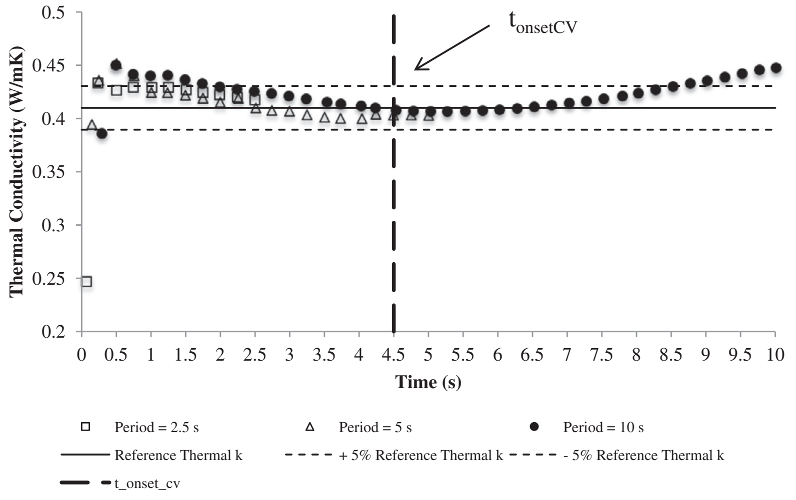

Fig. 13. Thermal conductivity of 50/50 DI water/Ethylene Glycol at 295 K and $P_0 = 0.15$ W.

is difficult to resolve when the solution maintains reasonable accuracy (±10% of the reported value).

3.2. Effect of known volumetric heat capacity and the onset of natural convection on methodology accuracy

As seen in Figs. 3–8, the common TPS methodology suffers from a difficulty in resolving the volumetric heat capacity of the fluid in close proximity to the sensor due to self-heating effects in the fluid. This results in the significant variations seen in the reported thermal conductivity of the fluid over short measurement intervals. Thus, it is predicted that when using a known value of heat capacity, the accuracy of the results will be improved during this early time interval. The known volumetric heat capacity is used with the sensor temperature measurements in Eq. (3)to solve for the thermal conductivity of each of the test fluids. The thermal conductivity is determined as a function of the final measurement time chosen by the user as well as the user-defined measurement period. The resulting distributions are presented in Figs. 9–14.

As seen in Fig. 9, the use of a known volumetric heat capacity in Eq. (3)collapses the reported data to within ±5% of the values for thermal conductivity that are reported in the literature. This is in stark contrast to the use of this method when the volumetric heat capacity of the fluid is unknown (Fig. 3). Thus, it is highly recommended that the volumetric heat capacity of the fluid be tested in advance and utilized as a known input when using the transient plane source technique for determining a fluid's thermal conductivity.

Fig. 9(a)–(d) also clearly indicate the effect of limiting the measurement time to the period in which natural convection is not significant. In these figures, the time at which convection begins over the sensor face demarcates the point at which the solution for the thermal conductivity of the fluid begins to rapidly increase. This highlights a significant limitation of the conventional methodology. For instance, if the measurement time is determined to be the point at which the thermal conductivity of DI water at 290 K is accurate ($t = 4.71$ s ($t_{onsetCV}$)) for all other measurements of this fluid, the calculated thermal conductivity for DI water at 320 K would be 25% higher than the value that is reported in the literature. Thus, even if the volumetric heat capacity of the fluid were known, the conventional methodology still may not yield an accurate calculation of a fluid's thermal conductivity.

For completeness, each of the remaining test fluids in Table 2 are measured using the method with known volumetric heat capacity and the thermal conductivity of each is reported in Figs. 10–14. In each of Figs. 10–14, the thermal conductivity data are shown to collapse around the values reported in Table 2. This confirms that advanced knowledge of the volumetric heat capacity of each fluid results in increased accuracy. Additionally, Figs. 10–14again confirm the importance of avoiding natural convection during the experiment. It should be noted that while there is still an initial period of time over which the solution is inaccurate (outside of 5% accuracy), this period has been substantially reduced when compared to Figs. 3–8. This initial inaccuracy is a direct result of too few data points over a short duration of time, making it difficult to apply a linear regression to the distribution described by Eqs. (3) and (4).

3.3. Effect of sensor temperature rise

One of the important user-defined parameters for determining the thermal conductivity of materials using the TPS instrument is the power loading level of the sensor. In one sense, the power loading level should be low for measuring the thermal conductivity of fluids using the TPS instrument in order to extend the time over which heat conduction dominates the solution to Eq. (3). However, a low power loading level results in a sensor temperature difference that is on the order of the temperature drift (i.e. the change in the fluid temperature due to minor changes in ambient conditions), resulting in an excessive amount of data scattering in ΔT as a function of time. It was determined that power loading levels below 0.05 W result in significant data scattering for all of the fluids in Table 2.

In order to determine the effect of sensor temperature rise on the thermal conductivity of the surrounding fluid in the absence of natural convection, Eq. (6)was used to predict the onset of natural convection across the sensor face for three fluids (DI water, Ethylene Glycol, Glycerin) as a function of power loading level (0.05–0.25 W in 0.05 W increments). Additionally, the known volumetric heat capacity of each of the three fluids was used to calculate thermal conductivity in order to guarantee an accurate solution. Finally, the final measurement time was chosen to be the time step immediately before $t_{onsetCV}$ for each of the fluids. By using the aforementioned criteria, the effect of sensor temperature rise on the calculated thermal conductivity is isolated. Each of the fluids is tested 5 times at each of the power loading levels and the thermal conductivity of each of the fluids is reported as a function of temperature and power loading level in Figs. 15–17.

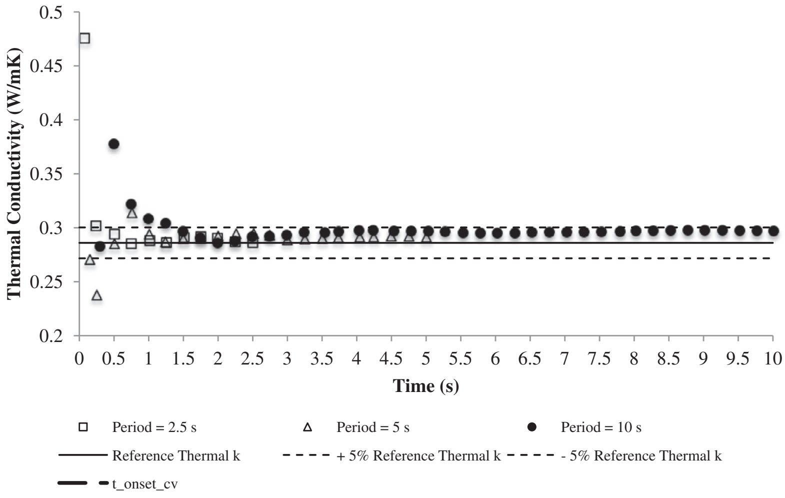

Fig. 14. Thermal conductivity of Glycerin at 295 K at $P_0 = 0.05$ W.

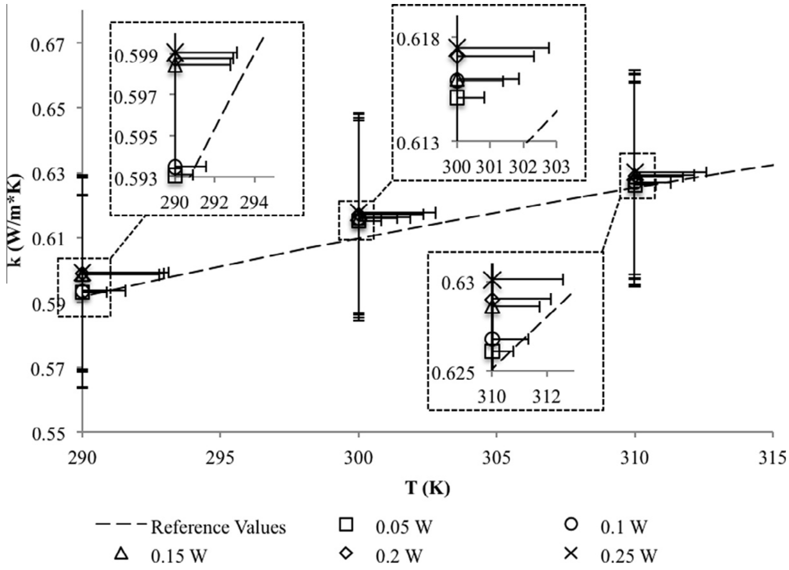

Fig. 15. Thermal conductivity of deionized water as a function of temperature and sensor power loading level P_0 compared to reference values in [32].

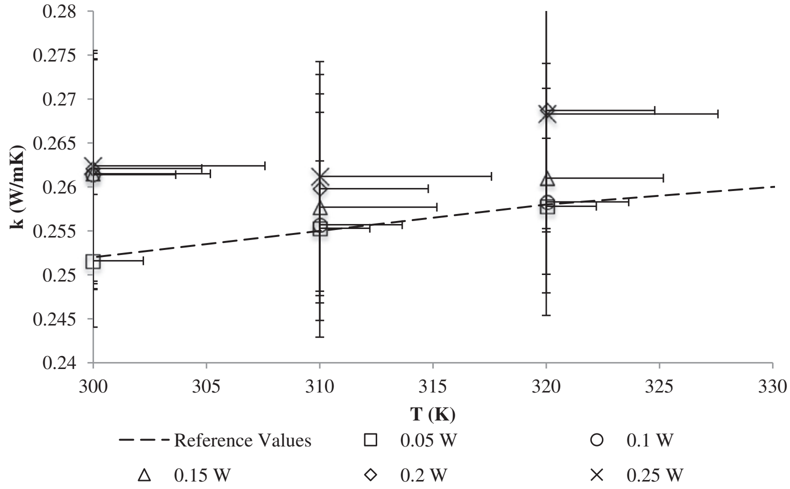

Fig. 16. Thermal conductivity of Ethylene Glycol as a function of temperature and sensor power loading level P_0 compared to reference values in [32].

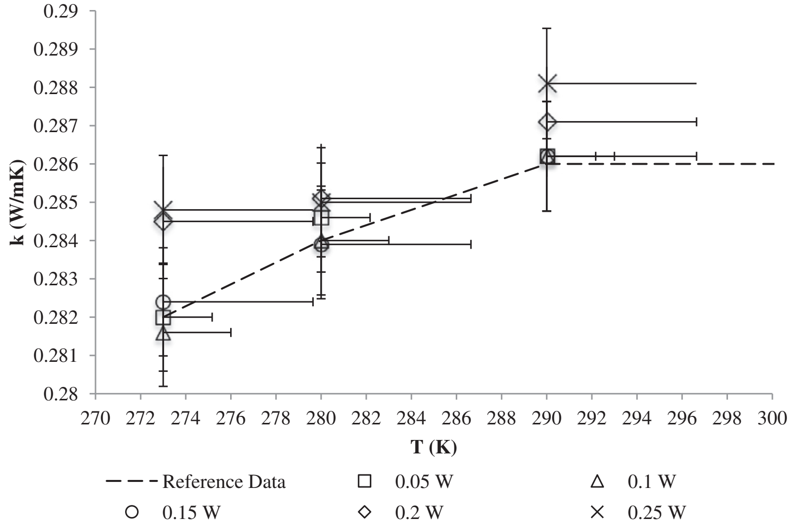

Fig. 17. Thermal conductivity of Glycerin as a function of temperature and sensor power loading level P_0 compared to reference values in [32] (Reproduced from [31]).

The vertical error bars in each of Figs. 15–17 represent the standard error calculated using each of the 5 experiments used to determine thermal conductivity, while the horizontal bars represent the average temperature rise of the sensor. Fig. 17 is a reproduction of Fig. 10 from [31] and is shown here for simple comparison against Figs. 15 and 16.

Figs. 15–17 reveal the sensitivity of the measurement to the power loading level of the sensor, P_0. In all cases, higher power loading levels generally over predict the thermal conductivity of the fluid. When one closely examines the temperature rise across the sensor at these power-loading levels, it is evident that the reported thermal conductivity is closer to the thermal conductivity at the maximum average temperature of the sensor. Based on the data presented in Figs. 15–17, it is recommended that the temperature rise across the sensor be kept to less than half of the temperature intervals over which the thermal conductivity of the fluid is measured. For instance, if the thermal conductivity of the fluid is determined using intervals of 10 K, the sensor temperature rise should not exceed 5 K.

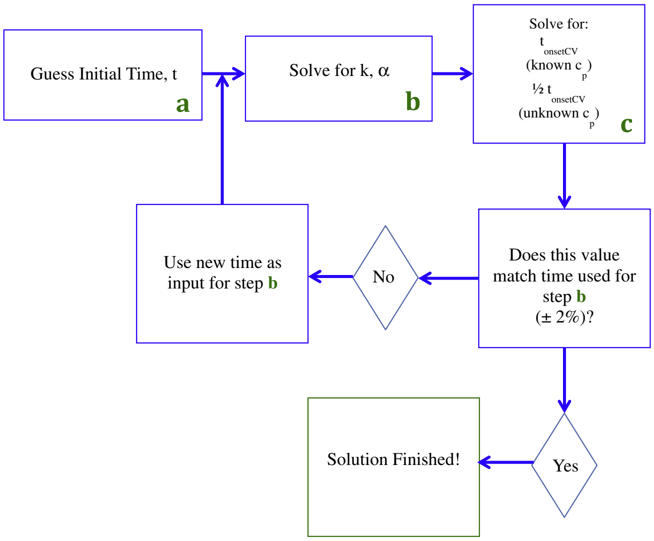

Fig. 18. New procedure used to determine the thermal conductivity of fluids with the TPS instrument.

3.4. Development of an accurate and repeatable methodology for determining the thermal conductivity of fluids using the TPS instrument

Because the thermal conductivity of the fluid is typically unknown prior to testing, it is difficult to determine whether the solution is accurate by simply plotting the distributions of thermal conductivity as a function of measurement time. Instead, two simple iterative solution procedures are developed here to determine the thermal conductivity of fluids when the volumetric heat capacity is both known and unknown.

The procedure proposed to determine the thermal conductivity of fluids using the TPS thermal characterization technique is outlined in Fig. 18.

For the new measurement methodology, a measurement time that corresponds to the time just prior to when natural convection begins yields the most accurate results for thermal conductivity when volumetric heat capacity is known *a priori* as seen in Figs. 9–14. In other words, the thermal conductivity of the fluid should be measured at the time period just prior to $t_{onsetCV}$ in order to guarantee that the both the initial period of data scattering and the onset of natural convection are avoided.

Deionized water and ethylene glycol are used to demonstrate this proposed methodology over a range of temperatures. As seen in Table 5, the new solution procedure is able to obtain the thermal conductivity of deionized water to within 5% of reference values for temperatures ranging between 290 and 320 K. It is also seen that the iterative solution for the time to the onset of natural convection closely matches those that were obtained in Table 4. This is a further indication that the solution procedure yields an accurate result. Table 6 presents the thermal conductivity of ethylene glycol as a function of temperature resulting from the new procedure.

Table 5
Example of iteration procedure for DI water as a function of temperature and sensor power.

Fluid temperature (K)	P_0 (W)	$t_{onsetCV}$ (s)	Initial guess (t_{final}) (s)	Thermal conductivity, *k* (W/m K)	Calculated $t_{onsetCV}$ (s)	Percent difference in *k* between iterations	Percent difference in *k* from literature value [32] (%)
290	0.1	–	1	0.5896	4.77	–	1.40
		4.77		0.5961	4744.72	1.10%	0.32
		4.72		0.5960	4.72	0.02%	0.33
290	0.25	–	1	0.6060	2.25	–	1.34
		2.25		0.6062	2.26	0.03%	1.37
		2.26		0.6063	2.26	0.02%	1.39
300	0.1	–	1	0.6615	3.16	–	7.91
		3.16		0.6183	3.39	6.53%	0.86
		3.39		0.6177	3.39	0.10%	0.77
300	0.25	–	1	0.6672	1.93	–	8.84
		1.93		0.6213	2.12	6.88%	1.35
		2.12		0.6239	2.11	0.42%	1.78
310	0.1	–	1	0.6099	2.85	–	2.88
		2.85		0.6489	2.68	6.39%	3.33
		2.68		0.6344	2.74	2.23%	1.02
310	0.25	–	1	0.6532	1.68	–	4.01
		1.68		0.6484	1.69	0.73%	3.25
		1.69		0.6483	1.69	0.02%	3.23
320	0.1	–	1	0.6386	2.39	–	0.45
		2.39		0.6410	2.38	0.38%	0.15
		2.38		0.6411	2.38	0.02%	0.17
320	0.25	–	1	0.6534	1.46	–	3.22
		1.46		0.6375	1.50	2.43%	0.72
		1.50		0.6391	1.50	0.25%	0.32

Table 6
Example of iteration procedure for Ethylene Glycol as a function of temperature and sensor power P_0.

Fluid temperature (K)	P_0 (W)	$t_{onsetCV}$ (s)	Initial guess (t_{final}) (s)	Thermal conductivity, k (W/m K)	Calculated $t_{onsetCV}$ (s)	Percent difference in k between iterations	Percent difference in k from literature value [32] (%)
300	0.1	–	1	0.2422	6.61	–	3.89
		6.61		0.2712	5.88	11.97%	8.48
		5.88		0.2614	6.11	3.61%	4.56
300	0.25	–	1	0.2479	4.06	–	1.63
		4.06		0.2653	3.78	7.02%	6.12
		3.78		0.2624	3.83	1.21%	4.96
310	0.1	–	1	0.2473	6.12	–	3.40
		6.12		0.2597	5.82	5.01%	1.45
		5.51		0.2557	5.56	1.54%	0.12
310	0.25	–	1	0.2610	3.64	–	1.95
		3.64		0.2759	3.44	5.71%	7.77
		3.44		0.2680	3.56	3.26%	4.69
320	0.1	–	1	0.2537	5.68	–	2.05
		5.68		0.2701	5.33	6.46%	4.29
		5.33		0.2690	5.35	0.41%	3.86
320	0.25	–	1	0.2403	3.48	–	7.22
		3.48		0.2690	3.36	11.9%	3.86
		3.36		0.2660	3.41	1.12%	2.70

Table 7
Example of iteration procedure for Methanol, Acetone, 50/50 DI water/Ethylene Glycol and Glycerin at 295 K.

Fluid type	P_0 (W)	$t_{onsetCV}$ (s)	Initial guess (t_{final}) (s)	Thermal conductivity, k (W/m K)	Calculated $t_{onsetCV}$ (s)	Percent difference in k between iterations	Percent difference in k from literature value [32] (%)
Methanol	0.15	–	1	0.1839	2.51	–	9.48
		2.51		0.2091	2.21	13.70%	2.75
		2.21		0.2049	2.25	2.00%	0.68
Acetone	0.15	–	1	0.1671	1.98	–	4.43
		1.98		0.1748	1.89	4.61%	9.25
		1.89		0.1690	1.95	3.31%	5.63
50/50 DI/ EG	0.15	–	1	0.4010	4.60	–	2.19
		4.60		0.4038	4.57	0.69%	1.51
		4.57		0.4042	4.57	0.09%	1.41
Glycerin	0.05	–	1	0.2881	21.35	–	0.73
		21.35		0.2965	20.73	2.91%	3.60
		20.73		0.2943	20.89	0.74%	2.90

Table 8
Example of iteration procedure for DI water as a function of temperature when volumetric heat capacity is unknown.

Fluid temperature (K)	P_0 (W)	1/2 $t_{onsetCV}$ (s)	Initial guess (t_{final}) (s)	Thermal conductivity, k (W/m K)	Volumetric heat capacity (MJ/m^3 K)	Percent difference in volumetric heat capacity from literature value [32] (%)	Percent difference in k from literature value [32] (%)
290	0.25	–	1	0.5726	4.47	7.19	4.25
		1.21		0.5964	4.12	0.72	0.27
		1.09		0.6112	4.01	3.37	2.21
		1.05		0.6076	4.04	2.65	1.61
		1.06		0.6059	4.05	2.41	1.32
300	0.25	–	1	0.6680	3.64	12.50	8.97
		0.89		0.6761	3.59	13.49	10.29
		0.87		0.6771	3.58	13.73	10.46
310	0.25	–	1	0.6600	4.00	3.38	5.10
		0.80		0.6680	3.95	4.59	6.37
		0.79		0.6648	3.97	4.11	5.86
320	0.25	–	1	0.6931	3.79	8.23	8.23
		0.65		0.6759	3.89	5.81	5.54
		0.68		0.6709	3.92	5.08	4.76

Again, the calculated thermal conductivity remained within 5% of its reported value in each case.

Finally, Table 7 presents results using the proposed methodology for fluids with a wide range of Prandtl numbers. The data are in excellent agreement with the values reported in the literature in all cases. There is only one instance for which the solution procedure yields a result that is not within ±5% of the reported value in the literature. In this case, the thermal conductivity of Acetone was shown to be 5.63% greater than the reported value in the literature. However, the results in Fig. 12 suggest that Eq. (6)over predicts the time to the onset of convection for acetone, possibly due to its high evaporation rate. This can result in small (but significant) fluid motion across the face of the sensor, resulting in an earlier than expected divergence from the value of thermal conductivity reported in the literature. When working with fluids that exhibit high evaporation rates, one should select a low sensor power loading level (so as not to accelerate the evaporation rate), a small measurement period and a measurement vessel with as little area open to the ambient environment as possible.

In some cases, it is not possible to measure the volumetric heat capacity of the fluid of interest. As such, it is important to establish a procedure for determining the thermal conductivity of fluids with reasonable accuracy when their volumetric heat capacities are unknown. This is a challenging endeavor due to the difficulty in resolving the volumetric heat capacity using thermal gradients in close proximity to the heat source when solving Eq. (3)(as shown in Figs. 3–8). This can be avoided by selecting a longer measurement time; however, many heat transfer fluids undergo natural convection rather quickly, even at low sensor power levels. Thus, it is important to select a point that is in between these two time constraints. The midpoint between these two times is proximate to ½ $t_{onsetCV}$ based on the data in Figs. 3–8. Using this data and the procedure outlined above, the new procedure used for determining the thermal conductivity of fluids with unknown volumetric heat capacity is demonstrated in Tables 8–10. It should be noted that for $T = 290$ K in Table 8, the solution is iterated beyond the point at which successive iterations produce ½ $t_{onsetCV}$ within 5% of each other in order to give the reader confidence that the solution continues to converge with successive iterations.

Table 9

Example of iteration procedure for Ethylene Glycol as a function of temperature and sensor power P_0 when volumetric heat capacity is known.

Fluid temperature (K)	P_0 (W)	1/2 $t_{onsetCV}$ (s)	Initial guess (t_{final}) (s)	Thermal conductivity, k (W/m K)	Volumetric heat capacity (MJ/m^3 K)	Percent difference in volumetric heat capacity from literature value [32] (%)	Percent difference in k from literature value [32] (%)
300	0.1	–	1	0.2703	2.64	1.49	7.26
		2.92		0.2827	2.53	5.60	12.18
		2.69		0.2832	2.53	5.60	12.38
		2.69		0.2832	2.53	5.60	12.38
300	0.25	–	1	0.2361	3.07	14.13	6.31
		2.35		0.2624	2.74	2.24	4.13
		1.93		0.2537	2.84	5.97	0.67
		2.05		0.2614	2.75	2.61	3.73
		1.95		0.2568	2.80	4.48	1.90
		2.02		0.2595	2.77	3.36	2.98
		1.98		0.2572	2.79	4.10	2.06
310	0.1	–	1	0.3006	2.45	9.93	17.88
		2.31		0.2892	2.60	4.41	13.41
		2.52		0.2830	2.64	2.94	10.98
		2.60		0.2811	2.66	2.21	10.24
		2.63		0.2802	2.67	1.84	9.88
		2.65		0.2803	2.67	1.84	9.92
310	0.25	–	1	0.2361	3.07	12.87	7.41
		2.20		0.2632	2.72	0.15	3.22
		1.80		0.2538	2.84	4.41	0.47
		1.93		0.2568	2.80	2.94	0.71
		1.89		0.2537	2.84	4.41	0.51
320	0.1	–	1	0.2668	2.97	8.00	3.41
		2.85		0.2814	2.79	1.45	9.07
		2.57		0.2827	2.78	1.09	9.57
		2.56		0.2861	2.74	0.36	10.89
320	0.25	–	1	0.2696	2.98	8.36	4.50
		1.78		0.2464	3.28	19.27	4.50
		2.09		0.2461	3.28	19.27	4.61

Table 10

Example of iteration procedure for Methanol, Acetone, 50/50 DI water/Ethylene Glycol and Glycerin at 295 K when volumetric heat capacity is unknown.

Fluid type	P_0 (W)	1/2 $t_{onsetCV}$ (s)	Initial guess (t_{final}) (s)	Thermal conductivity, k (W/m K)	Volumetric heat capacity (MJ/m^3 K)	Percent difference in volumetric heat capacity from literature value [32] (%)	Percent difference in k from literature value [32] (%)
Methanol	0.15	–	1	0.2107	2.05	1.49	2.83
		1.11		0.2146	2.01	0.50	4.73
		1.07		0.2136	2.03	0.50	4.25
Acetone	0.15	–	1	0.1740	1.60	4.76	8.75
		0.91		0.1738	1.61	4.17	8.63
		0.92		0.1744	1.60	4.76	9.00
50/50 DI/EG	0.15	–	1	0.3442	4.26	23.84	14.84
		3.15		0.3625	4.06	18.02	10.32
		2.88		0.3559	4.11	25.29	14.42
		2.96		0.3470	4.12	19.77	14.15
Glycerin	0.05	–	1	0.2719	3.23	6.60	7.61
		11.89		0.2961	3.07	1.32	0.75
		10.49		0.2960	3.08	1.65	0.58

In Table 8, a sensor power of 0.25 W is used in order to show that the new procedure maintains a reasonable accuracy even when the time to the onset of convection is short, which yields a very small duration of time for which an accurate solution exists. While not as accurate as when the volumetric heat capacity of the fluid is known, the solution accuracy for thermal conductivity is shown to be reasonable in comparison to other thermal characterization techniques [33–35] while also resolving the volumetric heat capacity of the fluid. In order to determine whether this solution method is valid for a wide range of fluids, each of the fluids in Table 2 is analyzed. In Table 9, the thermal conductivity of ethylene glycol is calculated as a function of both sensor power and temperature while Table 10 presents the thermal conductivities of the remaining fluids at room temperature.

In Table 9, the accuracy of the thermal conductivity of Ethylene Glycol is shown to depend on the sensor power of the TPS instrument. The accuracy is better with higher sensor powers due to the magnitude of the changes in the ambient temperature as compared to the sensor temperature rise. When a low power is used, the average sensor temperature rise is close in magnitude to the small changes in ambient temperature than at higher powers, resulting in a higher variability in the thermal conductivity over a longer period of time. This is contradictory to the results presented in Figs. 15–17, where the more accurate solution exists at lower sensor power levels. This result is likely due to the difficulty in resolving the heat capacity of the surrounding fluid in close proximity to the sensor; in this case, two different conditions must be satisfied simultaneously in order to accurately obtain both the heat capacity and the thermal conductivity: (1) the thermal conductivity must be obtained using a semi-infinite, conduction dominated boundary condition (i.e. as if the fluid were a solid) and (2) the heat capacity of the fluid must contain all of the pertinent degrees of freedom associated with freely rotating fluid molecules. This is one possible reason that the heat capacity appears to be more accurate for lower sensor power loading levels while the thermal conductivity appears to be more accurate at higher sensor power loading levels. Regardless, the new solution method achieves an accuracy of 15% or better overall temperatures at the sensor power levels of interest in this study (i.e. those which maintain a laminar flow regime over all fluid sets).

Table 10 shows that the solution maintains an accuracy of 15% or better for each of the remaining fluids. Due to the lack of significant analyses in the current literature, it is unknown to what degree this accuracy is an improvement over the current methodology; however, given the significant data scattering and the uncertainty surrounding the presence of convection during testing in the existing research, it is expected that the accuracy is correspondingly increased when the methodology established in this work is used. As expected, the fluid with the highest Prandtl number achieved the best accuracy due to the extended period of time prior to natural convection.

4. Conclusion

The conventional methodology used to determine the thermal conductivity of liquids with the transient plane source technique was evaluated and was found to yield unacceptable accuracies for a wide range of fluids when both thermal conductivity and volumetric heat capacity are unknown. This methodology was found to be acceptable when the volumetric heat capacity of the fluid is known *apriori*; however, the onset of natural convection in this case can still result in artificially high thermal conductivities if not properly accounted for.

As a result of the inaccuracies associated with the conventional methodology, a new methodology is developed in order to ensure an accurate and repeatable determination of the thermal conductivity of liquids using the TPS instrument. This methodology avoids the effects of natural convection during measurement and also avoids an initial time period during which the existing solution method cannot accurately resolve the volumetric heat capacity of the surrounding fluid and/or becomes non-linear due to the limited number of data points at small time scales.

The new solution methodology is tested for fluids having a wide range of Prandtl numbers when the volumetric heat capacity is both known and unknown. When the volumetric heat capacity is known, the new solution method is found to resolve the thermal conductivity of the surrounding fluid to within 5.6% of the values reported in the literature. When the volumetric heat capacity is unknown, the new solution procedure is able to obtain values for the surrounding fluids' thermal conductivities to within 15% of the values reported in the literature.

Acknowledgments

The authors wish to recognize the work done by undergraduate lab assistant Rebecca Weigand for support with the fabrication of test cells and materials acquisition. Her hard work is greatly appreciated. R.J.W. gratefully acknowledges support from the Environmental Protection Agency Science to Achieve Results (STAR) Fellowship.

This material is based upon work supported by the National Science Foundation under Grant No. 0931507. Any opinions, findings, and conclusions or recommendations expressed in this material are those of the author(s) and do not necessarily reflect the views of the National Science Foundation. The research described in this paper has also been funded in part by the United States Environmental Protection Agency (EPA) under the Science to Achieve Results (STAR) Graduate Fellowship Program. EPA has not officially endorsed this publication and the views expressed herein may not reflect the views of the EPA.

References

[1] G. Paul, M. Chopkar, I. Manna, P.K. Das, Techniques for measuring the thermal conductivity of nanofluids: a review, Renewable Sustainable Energy Rev. 14 (2010) 1913–1924.

[2] M. Wan, R.R. Yadav, K.L. Yadav, S.B. Yadaw, Synthesis and experimental investigation on thermal conductivity of nanofluids containing functionalized Polyaniline nanofibers, Exp. Therm. Fluid Sci. 41 (2012) 158–164.

[3] J. Xu, Y. Zou, M. Fan, L. Cheng, Effect of pore parameters on thermal conductivity of sintered LHP wicks, Int. J. Heat Mass Transfer 55 (9–10) (2012) 2702–2706.

[4] E. Solorzano, J.A. Reglero, M.A. Rodriguez-Perez, D. Lehmus, M. Wichmann, J.A. de Saja, An experimental study on the thermal conductivity of aluminum foams by using the transient plane source method, Int. J. Heat Mass Transfer 51 (25–26) (2008) 6259–6267.

[5] R. Heijl, D. Cederkrantz, M. Nygren, A.E.C. Palmqvist, Thermoelectric properties of $Ba_8Ga_{16}Ge_{30}$ with TiO_2 nanoinclusions, J. Appl. Phys. 112 (4) (2012) 044313.

[6] W. Wang, X. Yang, Y. Fang, J. Ding, J. Yan, Enhanced thermal conductivity and thermal performance of form-stable composite phase change materials by using β-aluminum nitride, Appl. Energy 86 (7–8) (2009) 1196–1200.

[7] J. Nanda, C. Maranville, S.C. Bollin, D. Sawall, H. Ohtani, J.T. Remillard, J.M. Ginder, Thermal conductivity of single-wall carbon nanotube dispersions: role of interfacial effects, J. Phys. Chem. C 112 (2008) 654–658.

[8] S.Y. Wu, H. Wang, S. Xiao, D.S. Zhu, An investigation of melting/freezing characteristics of nanoparticle-enhanced phase change materials, J. Therm. Anal. Calorim. 110 (2012) 1127–1131.

[9] V. Goyal, D. Teweldebrhan, A.A. Balandin, Mechanically-exfoliated stacks of thin films of Bi_2Te_3 topological insulators with enhanced thermoelectric performance, Appl. Phys. Lett. 97 (2010) 133117.

[10] J. Chen, X. Gui, Z. Wang, Z. Li, R. Xiang, K. Wang, et al., Superlow thermal conductivity 3D carbon nanotube network for thermoelectric applications, ACS Appl. Mater. Interface 4 (2012) 81–86.

[11] H. Nagai, F. Rossignol, Y. Nakata, T. Tsurue, M. Suzuki, T. Okutani, Thermal conductivity measurement of liquid materials by a hot-disk method in short-duration microgravity environments, Mater. Sci. Eng. A-Struct. 276 (2000) 117–123.

[12] T. Boumaza, J. Redgrove, Use of the transient plane source technique for rapid multiple thermal property measurements, Int. J. Thermophys. 24 (2003) 501–512.

[13] M. Gustavsson, S.E. Gustafsson, Thermal conductivity as an indicator of fat content in milk, Thermochim. Acta 442 (1–2) (2006) 1–5.

[14] G.A. Longo, C. Zilio, Experimental measurement of thermophysical properties of oxide–water nano-fluids down to ice-point, Exp. Therm. Fluid Sci. 35 (7) (2011) 1313–1324.

[15] L. Fan, J.M. Khodadadi, An experimental investigation of enhanced thermal conductivity and expedited unidirectional freezing of cyclohexane-based nanoparticle suspensions utilized as nano-enhanced phase change materials (NePCM), Int. J. Therm. Sci. 62 (2012) 120–126.

[16] B. Wright, D. Thomas, H. Hong, L. Groven, J. Puszynski, E. Duke, X. Ye, S. Jin, Magnetic field enhanced thermal conductivity in heat transfer nanofluids containing Ni coated single wall carbon nanotubes, Appl. Phys. Lett. 91 (2007) 173116.

[17] M. Gustavsson, E. Karawacki, S.E. Gustafsson, Thermal conductivity, thermal diffusivity, and specific heat of thin samples from transient measurements with hot disk sensors, Rev. Sci. Intstrum. 65 (12) (1994) 3856.

[18] V. Bohac, M.K. Gustavsson, L. Kubicar, S.E. Gustafsson, Parameter estimations for measurements of thermal transport properties with the hot disk thermal constants analyzer, Rev. Sci. Instrum. 71 (6) (2000) 2452.

[19] S.E. Gustafsson, B. Suleiman, N.S. Saxena, I. ul Haq, Transient plane source technique: experimental design criteria, High Temp-High Press. 23 (3) (1991) 289–293.

[20] V. Goyal, A.V. Sumant, D. Teweldebrhan, A.A. Balandin, Direct low-temperature integration of nanocrystalline diamond with GaN substrates for improved thermal management of high-power electronics, Adv. Funct. Mater. 22 (7) (2012) 1525–1530.

[21] Y. He, Rapid thermal conductivity measurement with a hot disk sensor. Part I. Theoretical considerations, Thermochim. Acta 436 (1–2) (2005) 122–129.

[22] S.E. Gustafsson, TTransient plane source techniques for thermal conductivity and thermal diffusivity measurements of solid materials, Rev. Sci. Tnstrum. 62 (3) (1991) 797–804.

[23] S.E. Gustafsson, E. Karawacki, M.N. Khan, Transient hot-strip method for simultaneously measuring thermal conductivity and thermal diffusivity of solids and fluids, J. Phys. D. Appl. Phys. 12 (9) (1979) 1411–1421.

[24] H. Zhang, Q. Wu, J. Lin, J. Chen, Z. Xu, Thermal conductivity of polyethylene glycol nanofluids containing carbon coated metal nanoparticles, J. Appl. Phys. 108 (2010) 124304.

[25] D. Zhu, X. Li, N. Wang, X. Wang, J. Gao, H. Li, Dispersion behavior and thermal conductivity characteristics of Al_2O_3 nanofluids, Curr. Appl. Phys. 9 (1) (2009) 131–139.

[26] P. Hu, W.-L. Shan, F. Yu, Z.-S. Chen, Thermal conductivity of AlN-ethanol nanofluids, Int. J. Thermophys. 29 (6) (2008) 1968–1973.

[27] S.Y. Wu, H. Wang, S. Xiao, D.S. Zhu, An investigation of melting/freezing characteristics of nanoparticle-enhanced phase change materials, J. Therm. Anal. Calorim. 110 (3) (2012) 1127–1131.

[28] N. Nikkam, M. Saleemi, M.S. Toprak, S. Li, M. Muhammed, E.B. Haghighi, R. Khodabandeh, B. Palm, Novel nanofluids based on mesoporous silica for enhanced heat transfer, J. Nanopart. Res. 13 (11) (2011) 6201–6206.

[29] G.H. Zhang, C.Y. Zhao, Thermal and rheological properties of microencapsulated phase change materials, Renewable Energy 36 (11) (2011) 2959–2966.

[30] http://www.hotdiskinstruments.com/applications/examples/liquids.html, Accessed: 6/19/2013.

[31] R.J. Warzoha, A.S. Fleischer, Determining the thermal conductivity of liquids using the transient hot disk method. Part I: Establishing transient thermal-fluid constraints, in press.

[32] E.W. Lemmon, M.L. Huber, M.O. McLinden, NIST Standard Reference Database 23: Reference Fluid Thermodynamic and Transport Properties-REFPROP, Version 9.0, National Institute of Standards and Technology, Standard Reference Data Program, Gaithersburg, 2010.

[33] S.M.S. Murshed, Simultaneous measurement of thermal conductivity, thermal diffusivity and specific heat of nanofluids, Heat Transfer Eng. 33 (8) (2012) 722–731.

[34] X. Zhang, H. Gu, M. Fujii, Experimental study on the effective thermal conductivity and thermal diffusivity of nanofluids, Int. J. Thermophys. 27 (2) (2006) 569–580.

[35] J.J. Healy, J.J. de Groot, J. Kestin, The theory of the transient hot-wire method for measuring thermal conductivity, B+C 82 (2) (1976) 392–408.